AEJ
Alexandria Engineering Journal

Performance of electric vehicle driven by a switched reluctance motor

A.A. Abd El-Salam and Mohamed A. El-khazendar
Electrical Power and Mechines Eng. Dept., Faculty of Eng., Tanta University, Tanta, Egypt

This paper discusses a simulation and modeling modules of proposed Electric Vehicle (EV) system configuration by creating components as individual subsystems that can be used interchangeably as embedded systems. EV system proposed model is composed of detailed models of four major types of components: electric motor, EV system controller, physical links, and vehicle dynamics. These modules were modeled in the Matlab/Simulink software. Dynamic model of a Switched Reluctance Motor (SRM) is investigated and then simulated. In addition, an EV is modeled and investigated. Finally, EV and SRM are physically linked and controlled with a proposed technique. This technique depends on the control of SRM with a multi-phase excitation instead of single-phase excitation to get the most distinct advantage of an electric vehicle that is quick and precise torque generation. Performance of EV system is simulated and analyzed with the two control methods. Simulation results for these two control methods show EV system performance with a completely discussion and comparison.

يناقش هذا البحث تمثيل ووضع نماذج للوحدات المكونة لمنظومة السيارة الكهربية المقترحة وذلك عن طريق بناءها كمنظومات فرعية مستقلة والتى يمكن أن تستخدم بطريقة تبادلية مكونة منظومة متكاملة. فقد تم تكوين النموذج المقترح لمنظومة السيارة الكهربية تفصيليا من أربعة نماذج رئيسية: نموذج للمحرك الكهربي، حاكم المنظومة، الرابط بين المكونات الكهربية و الميكانيكية و أخيرا نموذج لديناميكية المركبة. وقد تم تمثيل هذه النماذج من خلال برنامج الماتلاب/سميولنك. فقد تم إستقصاء النموذج الديناميكي لمحرك الممانعة ذو التغذية المحوله ومن ثم تمثيله برمجيا. وقد تم أيضا تمثيل نموذج لديناميكية السيارة مع تمثيل الرابط الميكانيكي الذي يربطها بالمحرك الكهربي. وأخيرا قد تم التحكم في تلك المنظومة بأسلوب مقترح وهوالتحكم في محرك الممانعة ذو التغذية المحوله عن طريق تغذية أوجه متعددة بدلا من تغذية وجه واحد وذلك للوصول إلي عملية توليد العزم السريع والدقيق والتي تعتبر أكثر صفه للسيارة الكهربية.وقد تم تمثيل وتحليل اداء منظومة السيارة الكهربية فى كلا الحالتين وقد تم مناقشة ومقارنة النتائج.

Keywords: Electric vehicle, Switched reluctance motor, Matlab/Simulink, Switching angles, Vehicle performance

1. Introduction

Electric vehicles are those powered by one or more energy storage systems that must be charged and recharged by a power source external to the vehicle. Recently a lot of Electric Vehicles (EV) had been developed [1] mainly to solve environmental and energy problems caused by the use of Internal Combustion engine Vehicles (ICV). Some of them already have enough performance even in practical use. However, they have not yet utilized the most remarkable advantage of EV. The generated torque of electric motors can be controlled much more quickly and precisely than that of internal combustion engines [2]. It is well known that the adhesion characteristics between tire and road surface are greatly affected by the control of traction motor. This means that the vehicle stability and safety can be greatly improved by controlling the motor torque appropriately. There are four categories of EV systems: The Battery EV (BEV), The Hybrid EV (HEV), the Fuel Cell EV (FCEV), and Ultra-capacitors, flywheels-based batteries [3]. Studies were conducted to analyze EV and HEV concepts [4– 5]. Several computer programs have been developed to describe the operation of EV and HEV trains, including: Simple EV simulation (SIMPLEV) from the DOE's Idaho National Laboratory [6], CarSim from AeroVironment Inc., JANUS from Durham University [7], ADVISOR from the DOE's National Renewable Energy Laboratory [8]. A Matlab-Based Modeling and Simulation Package for Electric

and Hybrid Electric Vehicle Design were developed [9]. In addition, the component models of the EV system were integrated in a Matlab-Simulink system simulation program [10]. Also, some traction control techniques were developed and realized utilizing electric motor's quick torque response [11]. A switched reluctance motor with a suitable design and control was used as a propulsion unit for EV [12- 14].

This paper presents a modeling and simulation modules based on Matlab/Simulink for electric vehicle system with emphasis on the propulsion unit and its controller. A Switched Reluctance Motor (SRM) has been Selected as the propulsion unit in this research, because of its high power density and excellent motor-load torque-speed matching characteristics. The developed simulation program will serve as an evaluation tool for SRM based EV designs and controls.

The paper is arranged as follows: The configuration of the newly developed electric vehicle system in SIMULINK is discussed first, followed by the description of features of the main simulation modules. These modules are an electric motor, EV system controller, transmission (i.e. electrical to mechanical links), and vehicle dynamics. Next, two control strategies, the normal technique is a single-phase excitation mode, and the proposed technique is a multi-phase excitation mode are introduced. The proposed control technique is suitable for obtaining the most distinct advantage of EV system. This advantage is the quick and precise toque generation to give a faster performance response. The complete vehicle simulation is then used to assess the performance of an EV such as acceleration ability, response for a driving cycles and braking. Simulation results for the two control methods show the SRM and EV performance with a complete discussion and comparison.

2. Design modeling, and simulation of an electric vehicle system

The overall electric vehicle system simulation is shown in fig. 1.

2.1. Electric vehicle dynamics modeling and simulation

Total tractive force F_{tot} is the force between the vehicle's tires and the road (parallel to the road) supplied by the propulsion unit. The tractive force must overcome the opposing forces that are summed together and labeled as the road load force F_{RL} [10, 15], and axle drag force F_a [16]. A summary of forces on a vehicle is shown in fig. 2. The vehicle dynamics model can be represented using the following equations:

$$K_m m \frac{dV_{XT}}{dt} = F_{TR} - F_a - F_{RL} . \quad (1)$$

$$F_{RL} = F_{gxT} + F_{roll} + F_{AD} . \quad (2)$$

$$F_a = \frac{T_a}{r} = \frac{b_a * \omega_a}{r} . \quad (3)$$

$$\omega_a = \frac{V_{XT}}{r} . \quad (4)$$

$$F_{TR} = \frac{T_{TR}}{r} . \quad (5)$$

$$\frac{dV_{XT}}{dt} = \frac{1}{K_m * m}\left[F_{TR} - \frac{b_a * \omega_a}{r} - m * g * \sin(\varphi) - \operatorname{sgn}(V_{XT})\left\{\begin{matrix} m * g * \left(C_o + C_1 V_{XT}^2\right) + \\ \frac{1}{2}\rho * C_D * A_f * (V_{XT} + V_o)^2 \end{matrix}\right\}\right] . \quad (6)$$

$$V_{XT} = \omega_a * r = \left(\frac{2 * \pi * N_m}{60 * GR}\right) * r . \quad (7)$$

The motion described by eq. (6) is the fundamental equation required for dynamic simulation of the vehicle system. Longitudinal vehicle dynamics subsystem simulation models the vehicle dynamic equation, with concentrated effect on one point, vehicle Center of Gravity (CG). The longitudinal force (Traction force) will be specified from propulsion unit, as well as the incline (Grade) angle ϕ, and a brake load torque on the wheels can be considered a set of Simulink

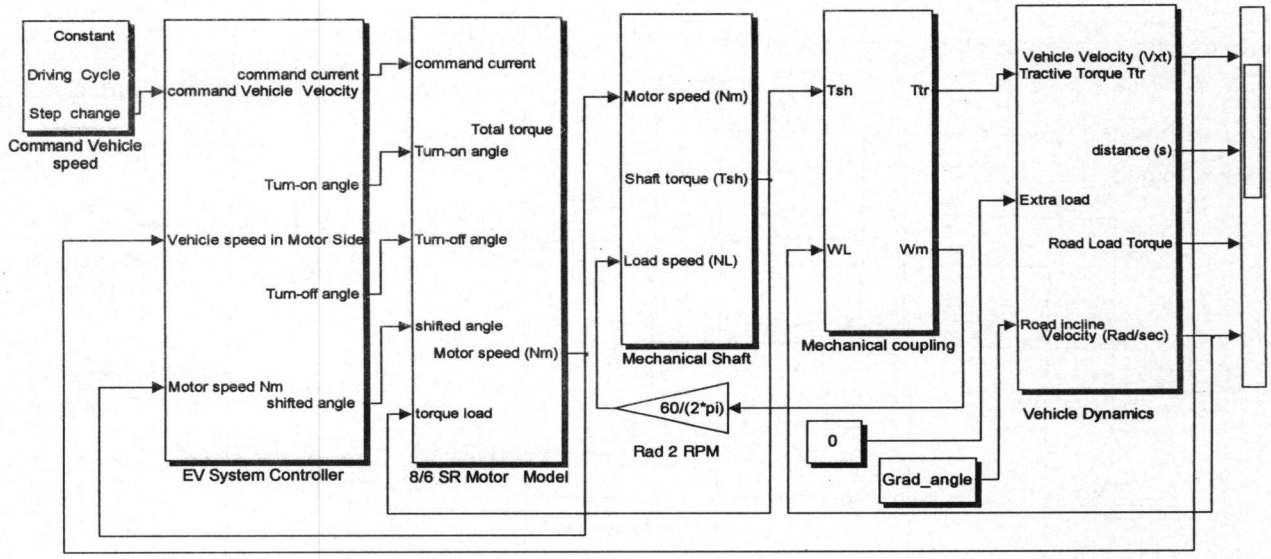

Fig. 1. Electric vehicle system simulation in SIMULINK.

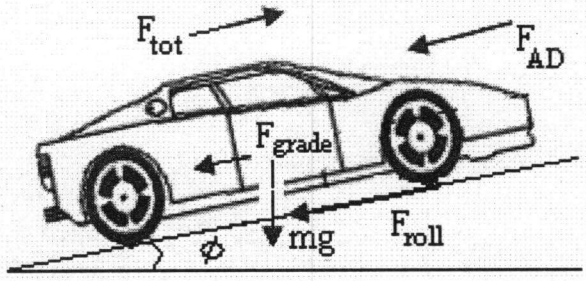

Fig. 2. A summary of forces on a vehicle.

input signals [10]. The simulation computes the vehicle velocity V_{XT}, axle shaft speed ω_a, and road distance s as a set of Simulink output signals. All signals are specified in SI units as shown in fig. 3.

A great advantage of an electrically driven propulsion system is the elimination of multiple gears to match the vehicle speed. The wide speed range operation of electric motors enabled by power electronics control, (as shown in next section), makes it possible to use a single gear ratio transmission for instantaneous matching of the available motor torque T_m with the desired tractive torque T_{TR}. The gear ratio can be calculated from maximum motor speed $N_{m,\max}$, maximum vehicle velocity $v_{\max}$ and wheel radius r using the following equation:

$$GR = \frac{\pi * N_{m,\max} * r}{30 * v_{\max}} = \frac{\pi * 600 * 0.1}{30 * 0.6} = 10.5. \quad (8)$$

2.2. Electric vehicle links

Electric vehicle links provides the connection between the electric motor and the vehicle dynamics module as shown in fig. 1.

2.2.1 Simulation of mechanical shaft

The Mechanical Shaft block is used to simulate a shaft interconnecting mechanically a motor drive block to a mechanical load block. Hence the Mechanical Shaft block allows decoupling of the mechanical parameters of the load from the ones of the motor. It represents an internal speed controller because it transfers the motor speed to tractive shaft torque. The mechanical shaft is represented by its stiffness coefficient K_{sh} and damping coefficient D_{sh} [17 and 18]. The shaft-transmitted torque T_{sh} is computed as:

$$T_{sh} = K_{sh} \int (\omega_m - \omega_l)\, dt + D_{sh} (\omega_m - \omega_l). \quad (9)$$

Where ω_m and ω_l are the speeds of the motor and the load, respectively. This is shown in fig. 4-a.

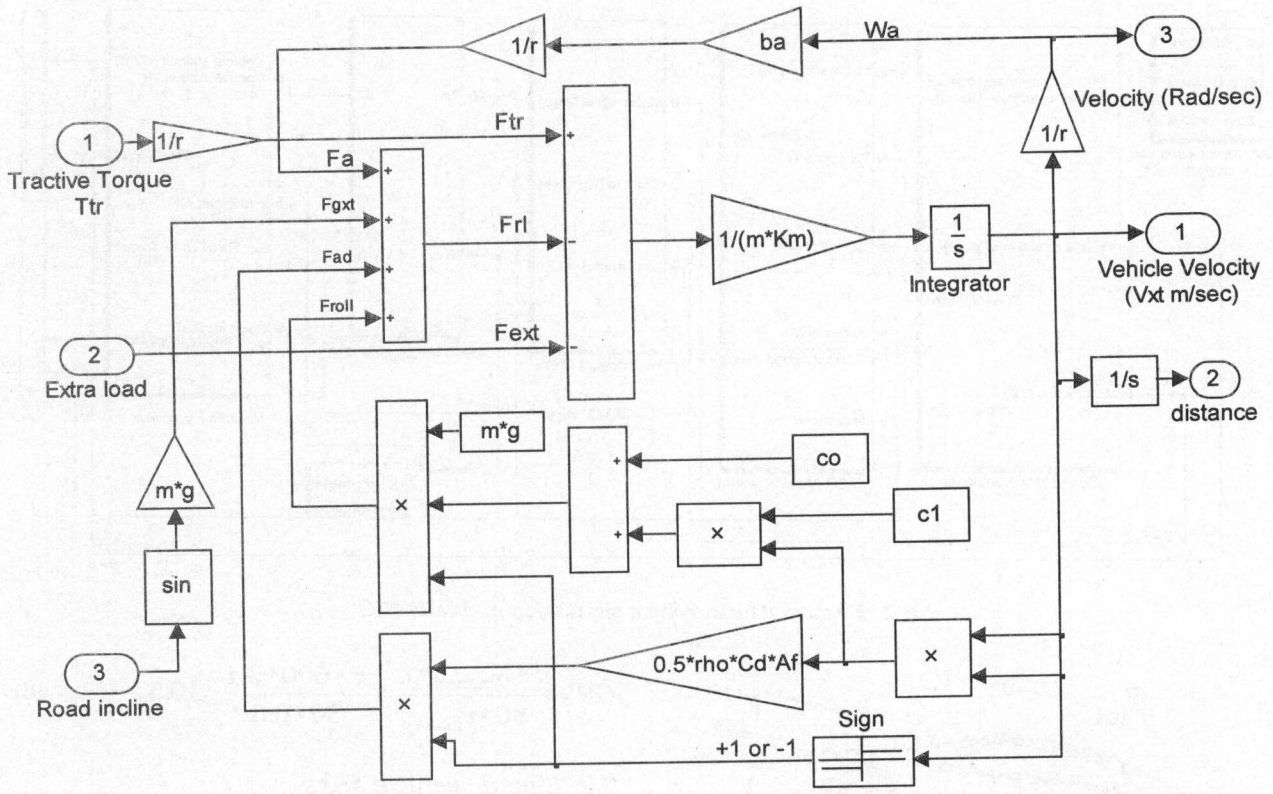

Fig. 3. The details of vehicle kinetics and roadway modeling (eq. (6)).

2.2.2. Simulation of mechanical coupling

The mechanical coupling is modeled as a simple gear with viscous drag torque [16]. As inputs, the coupling takes motor torque T_m and load speed ω_L. The outputs of the coupling are tractive torque T_{TR} and motor speed ω_m. Eqs. (10 and 11) are the equations for this component, while the corresponding SIMULINK code that implements the mechanical coupling is given in fig. 4-b.

$$T_{TR} = GR * (T_m - K\omega_m) \,. \tag{10}$$

$$\omega_m = GR * \omega_L \,. \tag{11}$$

Where, K is the viscous drag torque constant and GR is the gear ratio of the coupling.

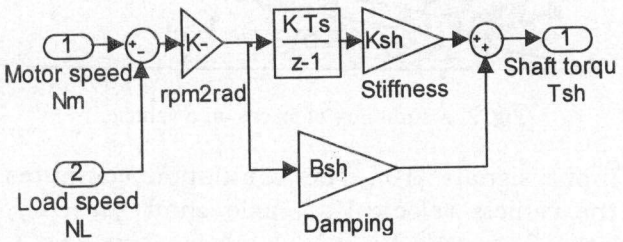

Fig. 4-a. Mechanical shaft block.

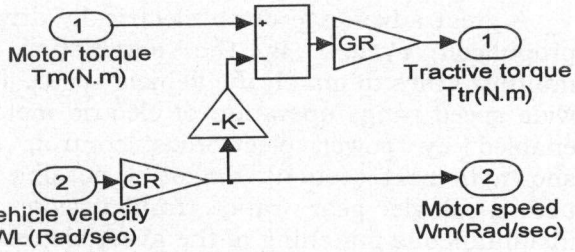

Fig. 4-b. Mechanical coupling block.

2.3. SRM model

A switched reluctance motor can be conveniently described by its flux-angle-current table and torque- angle- current table characteristics [19]. Either tables of these characteristics obtained from static measurements developed laboratory on the available 1 HP 8/6 SRM. Look-up tables are

used to store the machine's data. The flux-linkage can be obtained from the following equation:

$$\psi(\theta,i) = \int (V(\theta) - Ri)\, dt \,. \tag{12}$$

The phase current is obtained from the flux-angle-current look-up table. Then; the phase torque of SRM is obtained from torque-angle-current look-up table. The superposition of the individual phase torques gives the total electromagnetic torque T_e.

$$T_e = \sum_{j=1}^{m} T_{ph}\,(i_j, \theta_j). \tag{13}$$

The motor speed and rotor position is obtained from the following dynamic equations:

$$\omega_m = \frac{1}{J}\left(\int T_e - T_l - K\omega_m\right) dt \,. \tag{14}$$

$$\theta = \int \omega_m \, dt \,. \tag{15}$$

Fig. 5 illustrates the static torque versus different phase current and rotor positions for a typical SRM.

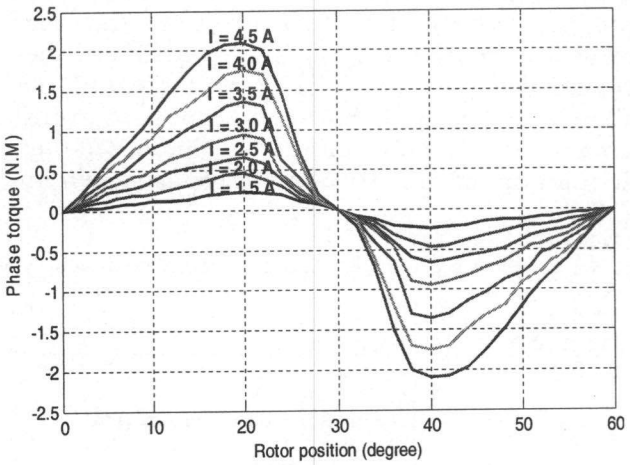

Fig. 5. SR motor phase static torque versus angular rotor position for various current levels.

2.4. EV system controller design and model

The controller model consists of four parts: PI speed controller, torque to current transformation, switching angles calculator, and a hysteresis current controller as shown in fig. 6 [19]. The vehicle speed V_{XT} is converted to motor rpm N_m using the gear ratio and wheel radius r as follow:

$$\omega_m = GR * (V_{XT}/r). \tag{16}$$

$$N_m = (60/(2 * \pi)) * \omega_m \,, \tag{17}$$

where, ω_m is the motor speed in rads/sec. Firstly, the output of the PI speed controller serves as the torque command input for the motor. The torque command in conjunction with the motor running speed sets up the control parameters for the electric motor. The control parameters for SRM are turn-on and turn-off angles for the phase excitation currents and the reference current. Secondly, the switching angle controller generates the control parameters that are used by all four phases. These parameters are determined by two control strategies: the first is the normal controller at which the turn-on and turn-off angles are fixed (single-phase excitation mode). The second is the proposed controller at which the turn-on angle is adapted (multi-phase excitation mode) depending on the command torque. The turn-on angle and the command current are predicted from the steady state simulation of SRM and the

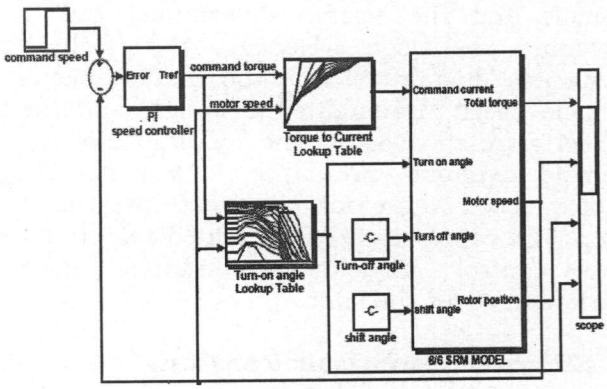

Fig. 6. SRM controller drive.

obtained data are stored on look-up tables. Maximizing the developed torque and extending the constant power region of SRM are obtained using the proposed controller to get the most distinct advantage of electric vehicle -quick and precise torque generation-. Lastly, hysteresis controller controls the phase current as shown in figs. 7- 10.

2.5. Integration and validation of the EV system

The simulation is configured in a feed-forward manner, where everything starts with the driver action see fig. 1. The vehicle driver determines the required vehicle velocity. The vehicle controller contains the switching logic that sends control signals to the SRM based on the feedback about vehicle operating conditions. This controller module allows the simulation to follow a prescribed vehicle speed schedule. The speed controller fulfills that role and provides the current demand signal based on the specified speed setting and the current vehicle speed. The torque is transmitted from motor to vehicle through two stages: the first is the torque generation from motor speed by using mechanical shaft controller, and the second is the torque conversion to vehicle side by using mechanical coupling. The final value at the wheel depends on transmission gear ratio (mechanical coupling) and the contribution of the electric motor, as well as on stiffness and damping of the drive shafts (mechanical shaft). The torque on the wheels is converted into tractive force, which in conjunction with other information about the vehicle and the terrain determines vehicle dynamic behavior. Hence, the vehicle dynamics module returns the instantaneous vehicle speed, transmitted distance, and the wheel angular velocity. The resultants of the vehicle dynamic simulation determine the motor speed value for the next integration step. The comparison of calculated results for two control modes demonstrates good performance for the later.

3. EV system performance analysis

The electric vehicle performance is demonstrated for both control methods. The minimum inductance position of SRM was taken as zero angle position ($\theta = 0°$) see fig. 5. The details were explained on [19]. The simulation was performed at fixed angles $\theta_{on} = 1°$ and $\theta_{off} = 16°$ (minimum switching angles) for single-phase excitation mode and θ_{on} is varied while; θ_{off} is fixed at 25° (maximum angle) for the proposed controller. The motor and vehicle specifications are listed in the appendix.

3.1. Electric vehicle driving cycle

The main motion types are the acceleration, cruising at constant speed, deceleration, and stopping of the vehicle. These motions can be tested by the complete driving cycle as a command vehicle velocity. Fig. 7 and 8 shows EV drive cycle at single-phase excitation mode and multi-phase excitation mode, respectively. Both of them has: (a) vehicle velocity, (b) SRM phase current, (c) SRM turn-on angle, (d) SRM torque, (e) vehicle transmitted distance, (f) motor torque and power vs. motor speed, (g) SRM phase current and voltage at low speed, and (h) SRM phase current and voltage at high speed. The time-vehicle performance relation is illustrated in table 1.

Simulation results presented here, show that the most distinct advantages of EV performance is obtained by using the proposed controller. It is obvious that the vehicle is accelerated rapidly. In addition, the capacity of vehicle velocity is increased as shown in (a). With the same phase current drawn, the motor torque is increased by adaptation of the turn- on angle as shown in

Table 1
Time-vehicle performance relation for complete driving cycle

Period(sec)	EV performance
0 : 1	stopping
1	Acceleration1
1 : 3.5	Acceleration1 time + cruising at 0.3 m/sec
3.5	Acceleration2
3.5 : 7	Acceleration2 time + cruising at maximum velocity
7 : 12	Deceleration + stopping

(b, c, and d). Then; the transmitted distance of the vehicle is increased (e). The speed and constant power region of SRM is extended (f). Finally, the corresponding motor current and voltage at low and high speeds are shown as in (g, and h).

3.2. *Braking and sudden change of torque operation*

Braking and sudden change of torque load is accomplished by an extra load that applied to vehicle as a force and also, by the shifted angle that delays the phase excitation. Fig. 9 and 10 shows the system performance with two control schemes. The time-vehicle performance relation at extra load and shifted angle is demonstrated in table 2.

Simulation results with the proposed controller present a good performance than with the normal controller. It is clearly from (a) that:

- The vehicle has a faster response to accelerate and reaccelerate (region 1and 5).
- The motor withstands the extra load torque (region 2) to drive the vehicle with constant speed.
- The vehicle has a faster response to the shifted angle (region 3and 4). In addition,
- The phase current rating is saved (b).
- The total motor current is increased due to increasing the conduction period (c).
- Motor torque is increased by turn-on angle adaptation (d and e).
- Traversed distance of the vehicle is increased (f).

Table 2
Time-vehicle performance relation at extra load and shifted angle

	Region 1	Region 2	Region 3	Region 4	Region 5
Time period (sec)	1:4.5	4.5:10	10:12	12:14	14:15
Extra Load (N)	0	60	60	60	0
Shifted angle (degree)	0°	0°	20°	30°	0°

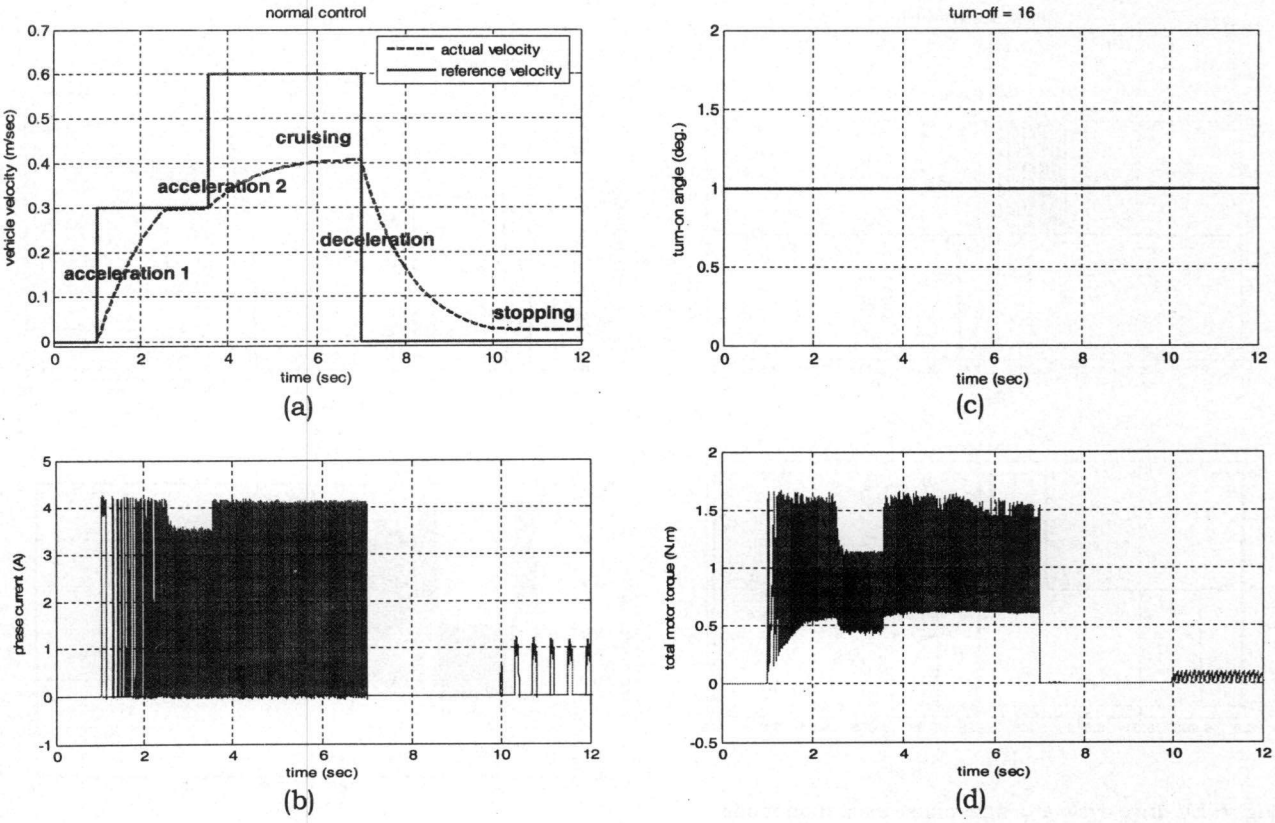

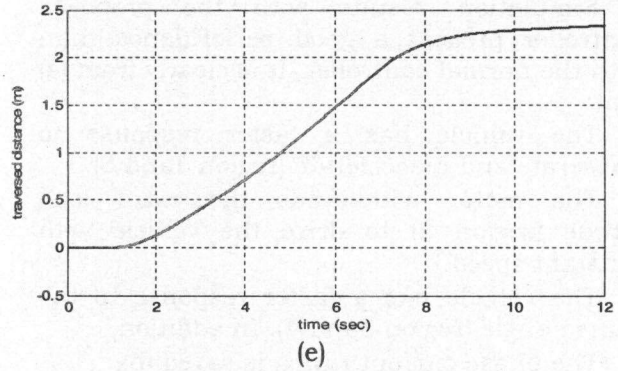

(e)

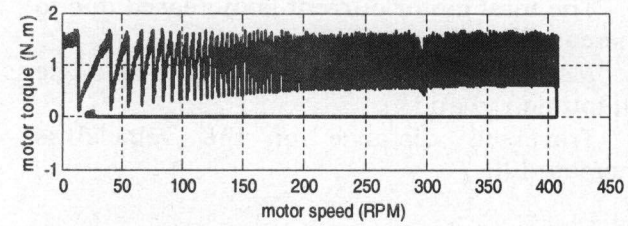

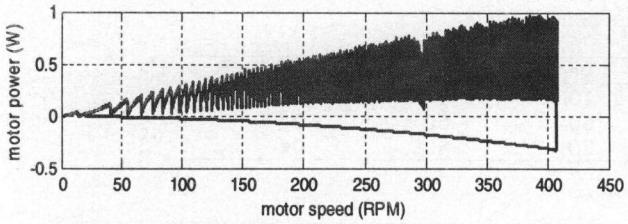

(f)

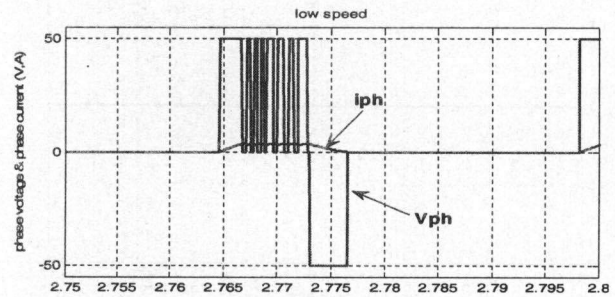

(g)

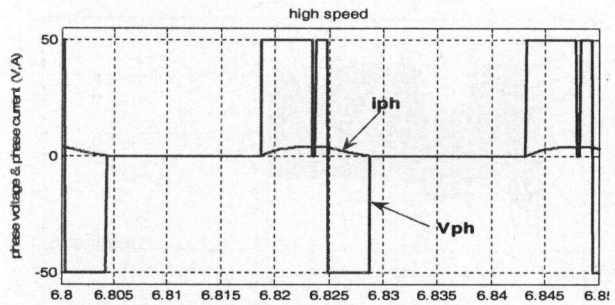

(h)

Fig. 7. EV drive cycle at single-phase excitation mode (normal controller).

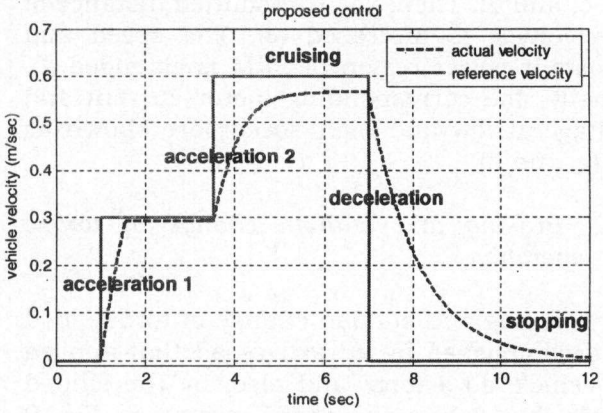

(a)

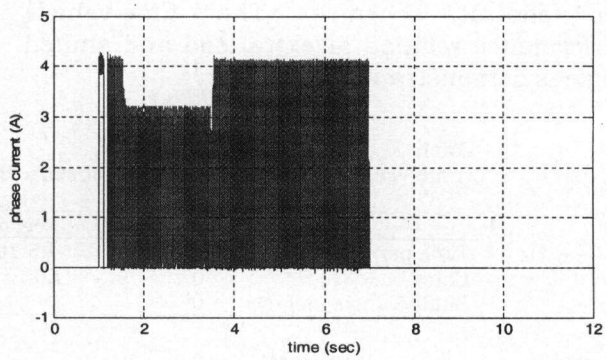

(b)

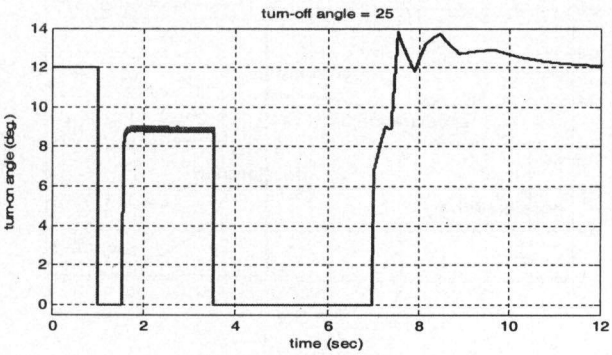

(c)

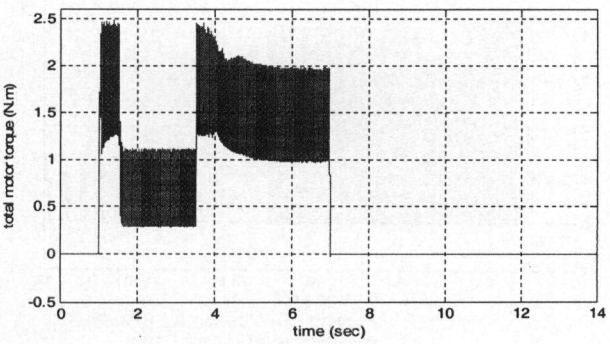

(d)

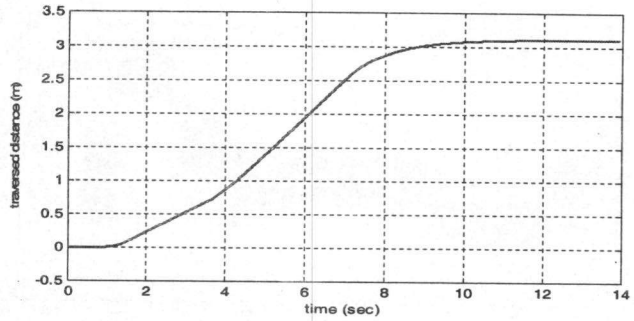

(e)

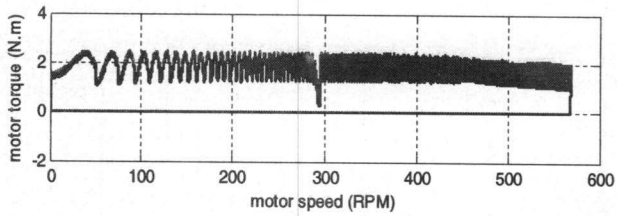

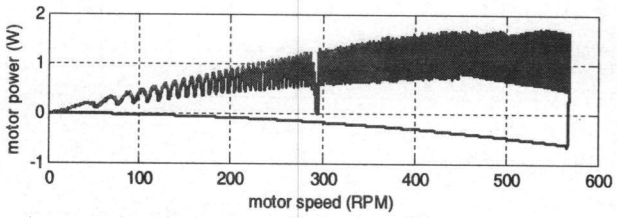

(f)

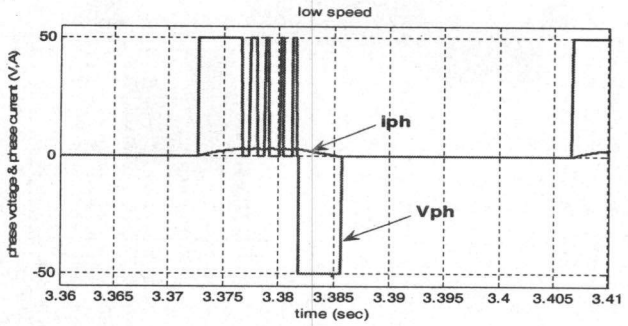

(g)

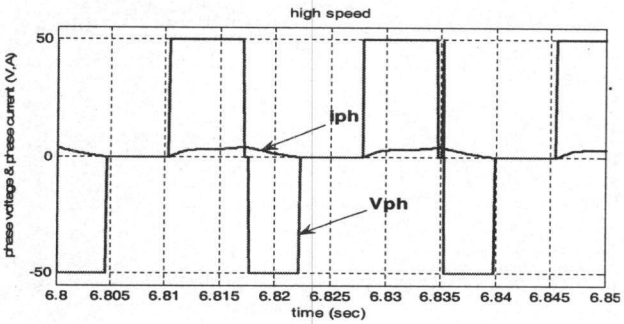

(h)

Fig. 8 EV drive cycle at multi-phase excitation mode (proposed controller).

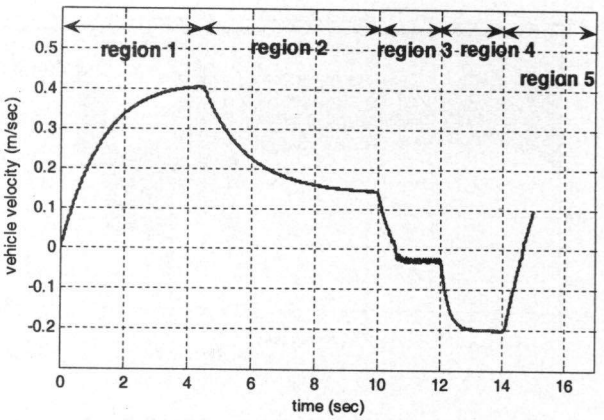

(a)

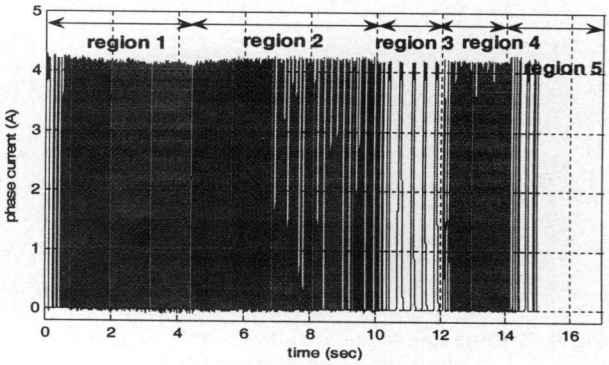

(b)

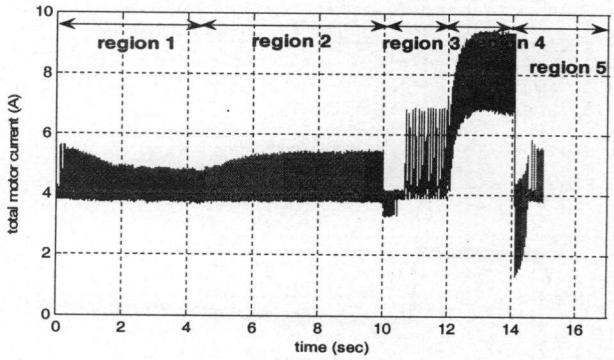

(c)

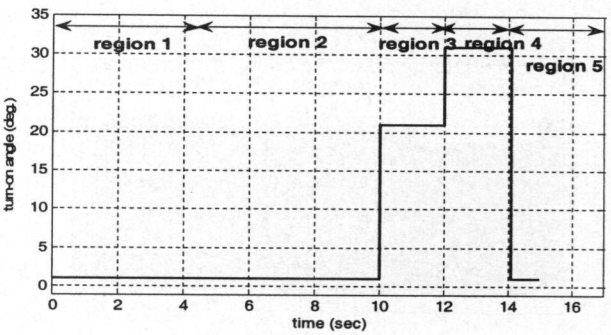

(d)

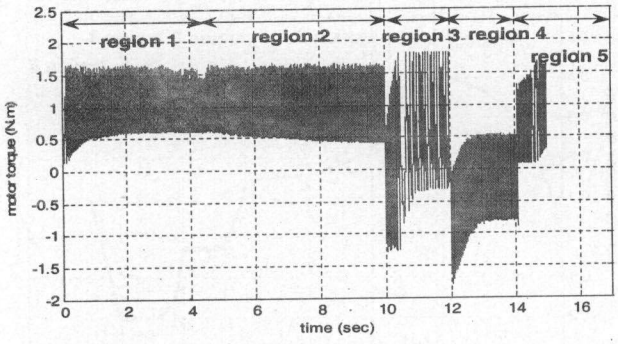

(e)

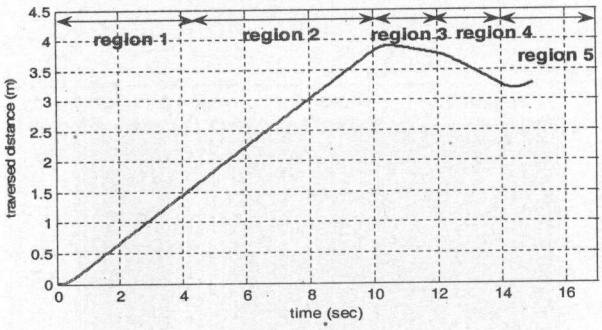

(f)

Fig. 9. Braking and sudden change of torque operation at single-phase excitation mode.

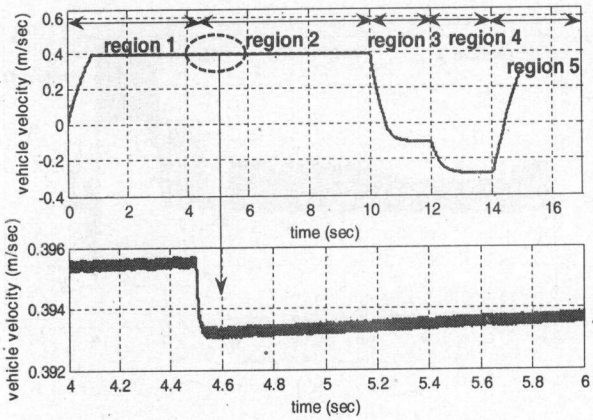

(a)

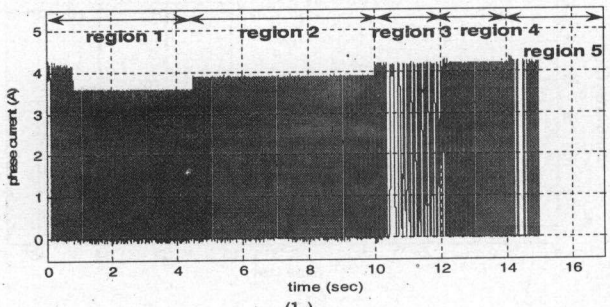

(b)

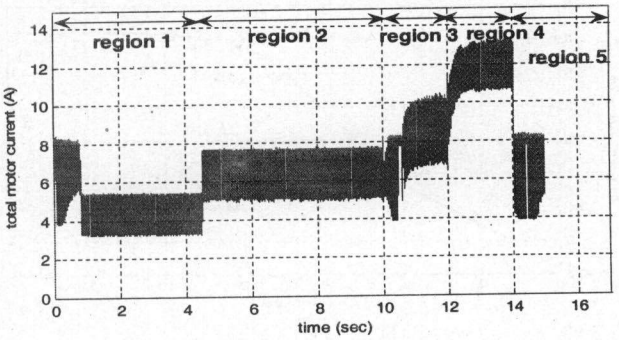

(c)

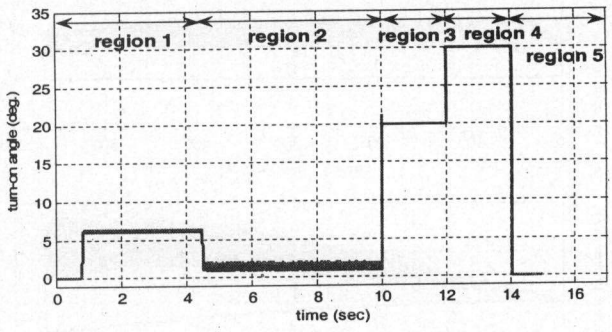

(d)

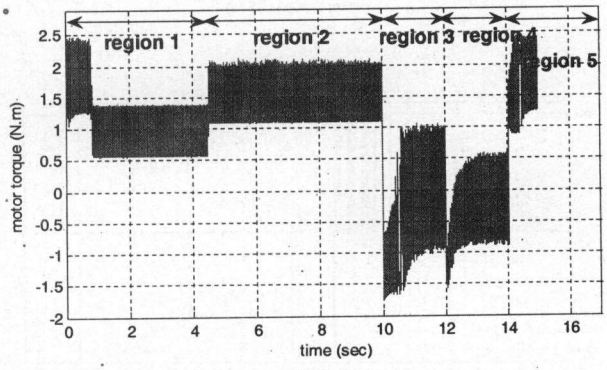

(e)

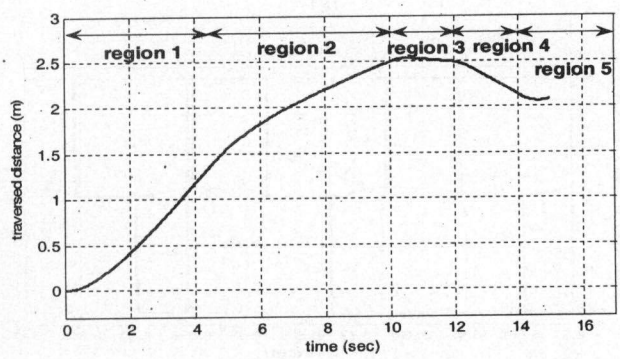

(f)

Fig. 10. Braking and sudden change of torque operation at multi-phase excitation mode.

4. Conclusions

Modeling and simulation of EV subsystem modules have been implemented individually. Then, the integration and validation of the complete EV system has been simulated in SIMULINK. SRM with two control methods has been used to drive the EV system. Initial acceleration, response to driving cycle, and braking have been implemented for both control methods. The obtained results suggested that the most distinct advantage of electric vehicle -quick and precise torque generation- can be obtained with appropriate control on the propulsion system.

Appendix

Vehicle model variables and constants

m is the total mass of the vehicle system (50 kg),

K_m is the Rotational inertia coefficient to compensate for the apparent increase in the vehicle's mass due to the onboard rotating mass: $1.08 =< K_m <= 1.1$,

V_{XT} is the Longitudinal road tangential vehicle velocity (m/s),

$\frac{dV_{XT}}{dt}$ is the acceleration of the vehicle (m/s^2)

F_{gxT} is the gravity force (N),

F_{roll1} is the dry friction or rolling resistance of the tires force(N),

F_{AD} is the aerodynamic drag force (N),

b_a is the axial shaft speed drag torque constant (0.3),

ω_a is the axle shaft speed (radian / sec),

g is the gravitational acceleration (9.81 m/s^2),

ϕ is the incline or grad angle (0^o or radian),

sgn is the +1 or -1

C_o is the the coefficient of rolling resistance, $0.004 =< C_o <= 0.02$,

C_1 is the unit less $<<< C_o$,

ρ is the mass density of air (1.225 kg/m^3),

C_D is the aerodynamic drag coefficient ($0.4 > C_d >= 0.2$ $N{\cdot}s^2/kg{\cdot}m$),

A_f is the effective frontal vehicle cross-sectional area (0.5 m^2),

V_o is the head-wind velocity (neglected here),

N_m is the motor speed (RPM), and

S is the tangential roadway distance (meter).

References

[1] K. Rajashekara, "History of Electric Vehicles in General Motors", IEEE Trans. on Ind. Appl., Vol. 30 (4), pp. 897-904 (1994).

[2] T. Furuya, Y. Toyoda and Y. Hori, "Implementation of Advanced Adhesion Control for Electric Vehicle", Proc. IEEE Workshop on Advanced Motion Control (AMC-Mie'96), Vol. 2, pp. 430- 435 (1996).

[3] C.C. Chan and Y.S. Wong, "Electric Vehicle Charge Forward", Power and Energy Agazine, November/December (2004).

[4] M. Hayashida et al., "Study on Series Hybrid Electric Commuter-Car Concept", SAE J. SP-1243, Paper 970197, Feb. (1997).

[5] L.J. Oswald and G.D. Skellenger, "The GM/DOE Hybrid Vehicle Propulsion Systems Program: A Status Report", in Proc. Electric Vehicle Symp. 15, Orlando, FL, Dec. (1997).

[6] G. Cole, "Simple Electric Vehicle Simulation (SIMPLEV) v3.1", DOE Idaho National Eng. Lab.

[7] J.R. Bumby et al., "Computer Modeling of the Automotive Energy Requirements for Internal Combustion Engine and Battery Electric-Powered Vehicles," Proc. Inst. Elect. Eng., Vol. 132, pt. A (5), pp. 265–279 (1985).

[8] K.B. Wipke and M.R. Cuddy, "Using an Advanced Vehicle Simulator (ADVISOR) to Guide Hybrid Vehicle Propulsion System Development," Available at: http://www.hev.doe.gov.

[9] L. Butler Karen and Mehrdad Ehsani, Preyas Kamath, "A Matlab-Based

Modeling and Simulation Package for Electric and Hybrid Electric Vehicle Design", IEEE Transactions on Vehicular Echnology, Vol. 48 (6) (1999).

[10] Iqbal Husain and Mohammad S. Islam, "Design, Modeling and Simulation of an Electric Vehicle System", the University of Akron (1999).

[11] Yoichi Hori, Yasushi Toyoda and Yoshimas a Tsuruoka "Traction Control of Electric Vehicle University of Tokyo, 7-3-1 Hongo, Bunkyo, Tokyo 113, Japan.

[12] M. Rahman Khwaja, and E. Schulz Steven " High-Performance Fully Digital Switched Reluctance Motor Controller for Vehicle Propulsion" IEEE Transations on Industry Applications, Vol. 38 (4) (2002).

[13] Z. Rahman, K.L. Butler and M. Ehsani "Effect of Extended-Speed, Constant-Power Operation of Electric Drives on the Design and Performance of EV-HEV Propulsion System" Texas A and M University (2000).

[14] S. Ramamurthy Shyam and Juan Carlos Balda, "Sizing a Switched Reluctance Motor for Electric Vehicles IEEE Transactions on Industry Applications, Vol. 37 (5) (2001).

[15] S. Sadeghi, J. Milimonfared, M. Mirsalim and M. Jalalifar. "Dynamic Modeling and Simulation of a Switched Reluctance Motor in Electric Vehicles", 0-7803-9514-X/06/$20.00 IEEE, University of Technology, Esfahan, Iran (2006).

[16] Troy Brendon Savoie, B.S.M.E., "Modeling and Control of a Series Configured Hybrid Electric Vehicle for Parametric study", Master of Science in Engineering, The University of Texas at Austin, August (1997).

[17] Norton and L. Robert, Machine Design, Prentice Hall (1998).

[18] Nise and S. Norman, Control Systems Engineering, Addison-Wesley Publishing Company (1995).

[19] A.A. Abd El-Salam, Mohamed A.El-Khazendar, "Dynamic Performance Analysis and Control of a Switched Reluctance Motor for Electric Vehicle Applications", Engineering Research Journal (ERJ), Vol. 30 (2), Faculty of Engineering, Shebin El-Kom, Minoufiya University, Egypt (2007).

Received February 27, 2007
Accepted June 3, 2007